

USING INFRARED COLORS TO IDENTIFY OBSCURED AGN

HANNAH MARLOWE & RYAN ALLURED

Department of Physics and Astronomy, University of Iowa, Iowa City, IA 52242

Draft version December 7, 2012

ABSTRACT

Mid-infrared radiation is able to penetrate the obscuring dust that hides AGN at particular viewing angles in other wavelengths, making the Wide-field Infrared Survey Explorer (WISE) a powerful tool in the search for active galactic nucleus (AGN) candidates. In this paper, a simple color selection criterion using only the 3.4 and 4.6 μm WISE bands is tested in the COSMOS field using a Spitzer two-color selection technique as a truth table. For the WISE color criterion, $[3.4] - [4.6] > 0.8$ (Vega magnitudes), we calculate a completeness and reliability of 78% and 94%, respectively. By comparing to the SDSS quasar catalog, a 4.68:1 ratio of obscured to unobscured AGN is determined. Multiwavelength properties of the WISE-selected AGN are also discussed.

Subject headings: Infrared: galaxies — galaxies: active — surveys — X-rays: diffuse background

1. INTRODUCTION

The X-ray background (XRB) is observed as isotropic, diffuse emission on the sky. It was first observed during a 1962 rocket flight (Giacconi et al. 1962), and later observations have verified the presence of this background behind resolvable point sources. The presence of a diffuse XRB suggests the possibility of a widespread high energy process at some earlier epoch, analogous to the hydrogen recombination which produced the cosmic microwave background. It is now thought, however, that the XRB can be attributed to distant, unresolved point sources (Seward & Charles 1995). Alternative theories have been proposed suggesting a truly diffuse XRB due to a hot intergalactic gas ($kT \sim 30$ keV). The existence of such a gas, however, would cause a distortion of the cosmic microwave background spectrum due to the inverse Compton effect. The perfect blackbody spectrum of the CMB measured by COBE rules out such possibilities (Fabian & Barcons 1992).

The ROSAT mission resolved approximately 70–80% of the 0.5–2 keV XRB into point sources (Hasinger et al. 1998). In the 2–8 keV band, Chandra and XMM-Newton deep field surveys have resolved $> 80\%$ of the XRB (Brandt & Hasinger 2005). Roughly 83% and 95% of these sources are classified as AGN in the 0.5–2 keV and 2–8 keV bands, respectively (Bauer et al. 2004). In fact, the XRB spectrum can be explained by the superposition of type I and type II AGN, where type I AGN have both broad and narrow line emission and type II exhibit only narrow line emission (Khachikian & Weedman 1974). The two classifications of AGN (types I and II) are thought to be the result of an obscuring dusty torus which absorbs the visible and UV radiation of the compact object and re-radiates in the mid-infrared (Rowan-Robinson 1977). Type II AGN are called obscured because they are inclined such that the dusty torus lies in the observer’s line-of-sight. The spectra of obscured AGN are harder than their unobscured counterparts due to absorption of soft X-ray photons in the dusty torus, and are required in larger numbers to fit the 20–30 keV peak of the XRB spectrum. The predicted distribution of AGN as a function of hydrogen column density based

on the Great Observatories Origins Deep Survey (Dickinson et al. 2003) is shown in Fig. 1, where the lower bound of 10^{20} cm^{-2} is due to the interstellar medium and the upper bound of 10^{25} cm^{-2} is due to observing the AGN directly through the dusty torus. Fig. 2 shows a well-fit XRB by a model assuming a fixed 3:1 ratio of obscured to unobscured AGN, where the obscured classification is defined by a hydrogen column density greater than 10^{22} cm^{-2} (Treister & Urry 2005). Other studies have assumed a ratio of obscured to unobscured AGN that declines with luminosity due to radiative evaporation of the obscuring torus (Madau et al. 1994; Comastri et al. 1995; Gilli et al. 1999; Pompilio et al. 2000), but most models agree that the ratio should be on the order of 3:1.

Worsley et al. (2005) analyzed Chandra and XMM-Newton deep fields and found that the unresolved fraction of the XRB spectrum is too hard to be explained by unobscured AGN, suggesting a large number of missing type II AGN in agreement with previous modeling. This is further supported by the fact that the resolved fraction of the XRB falls at higher energies, with only 50% being resolved at 10 keV. In order to definitively explain the origin of the XRB, it is necessary to find these “missing” AGN. It is widely accepted that most AGN selection methods are strongly biased toward unobscured AGN, particularly those in the soft (< 10 keV) X-ray band strongly affected by photoelectric absorption and Compton scattering. Potential avenues for overcoming this selection bias are surveys in the radio, mid-infrared (MIR), or hard (> 10 keV) X-ray bands (Stern et al. 2012). Due to the low fraction of radio-loud AGN (Stern et al. 2000) and the unavailability of hard X-ray telescopes with sufficient sensitivity and angular resolution, MIR surveys are the most promising tools to uncover the missing type II AGN population.

Because MIR suffers less extinction as compared to optical, NIR, and soft X-ray, both type I and type II AGN should be detectable in this band. A characteristic AGN energy spectrum is shown in Fig. 3, and contains a MIR thermal component due to the heated torus, as well as the “big blue bump” (BBB) associated with the thermal accretion disk emission. The spectrum of a typ-

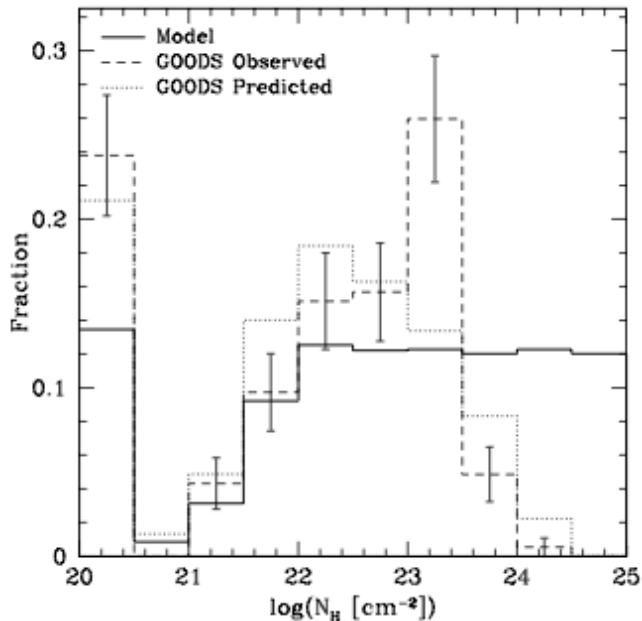


FIG. 1.— The distribution of AGN as a function of hydrogen column density based on observations from the Great Observatories Origins Deep Survey. The lower bound at 10^{20} cm^{-2} is due to absorption in the interstellar medium, and the upper bound at 10^{25} cm^{-2} is due to observing the AGN directly through the dusty torus.

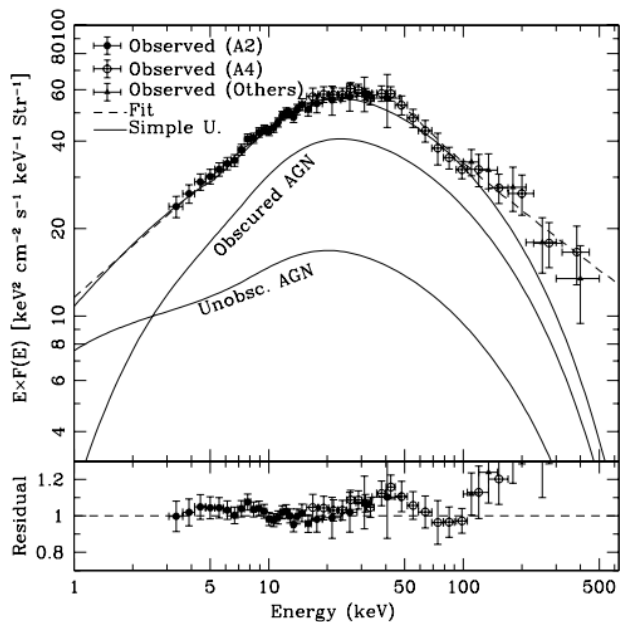


FIG. 2.— The simple population model of Treister & Urry (2005) compared to previous observations of the XRB. This model assumes a constant 3:1 ratio of obscured to unobscured AGN, independent of luminosity or redshift.

ical galaxy is a composition of stellar blackbodies which peaks at approximately $1.6 \mu\text{m}$, in between the two thermal bumps of the AGN spectrum. An AGN spectrum is predicted to be redder than an inactive galaxy due to the presence of the MIR thermal component, allowing one to differentiate AGN from normal galaxies (Stern et al.

2005). This is similar to the UV-excess method, which uses bluer colors predicted in the UV due to the BBB to differentiate active from inactive galaxies (Schmidt & Green 1983), but suffers less from extinction and avoids the Lyman α forest at high redshifts.

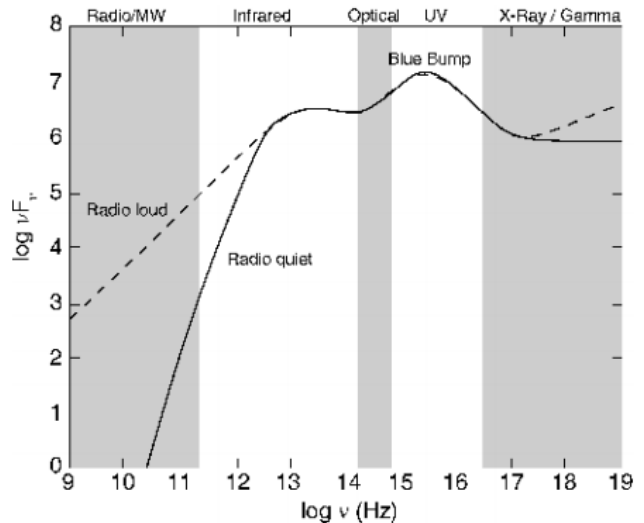


FIG. 3.— The AGN spectrum. The “big blue bump” is due to thermal accretion disk emission. A MIR bump is present due to thermal emission from the torus. (Schneider 2006).

Stern et al. (2005) completed a study of spectroscopically confirmed AGN in the 9 deg^2 Boötes field of the NOAO Deep Wide-Field Survey (NDWFS; Jannuzi & Dey (1999)) using the Infrared Array Camera (IRAC) Shallow Survey (Fazio et al. 2004) with the Spitzer Space Telescope (Werner et al. 2004). Fig. 4 shows a color-color plot of the sources of this study where the dotted line empirically separates active nuclei from Galactic sources and normal galaxies. They found the optimal color criteria to be

$$\begin{aligned} ([5.8] - [8.0]) &> 0.6 \wedge \\ ([3.6] - [4.5]) &> 0.2([5.8] - [8.0]) + 0.18 \wedge, \quad (1) \\ ([3.6] - [4.5]) &> 2.5([5.8] - [8.0]) - 3.5 \end{aligned}$$

where \wedge is the logical and symbol. The first restriction is necessary to exclude cool Galactic contaminants; the second excludes low-redshift inactive galaxies and stellar contaminants; and the third excludes high-redshift inactive galaxies. This simple mid-infrared color criteria selected over 90% of type 1 AGNs and 40% of type 2 AGNs spectroscopically identified by the AGN and Galaxy Evolution Survey (Stern et al. 2005; Kochanek et al. 2012).

Source confusion can be lessened by shallower observations that exclude high-redshift inactive galaxies. The Wide-Field Infrared Survey (WISE; Wright et al. (2010)) equatorial pointings, which are much shallower than most IRAC pointings, do not detect galaxies beyond $z \gtrsim 1.3$. Thus, in contrast to the selection criteria of Stern et al. (2005) above, a WISE color-criteria does not require the vertical restriction to eliminate high-redshift galaxies in the upper right of the color-color diagram.

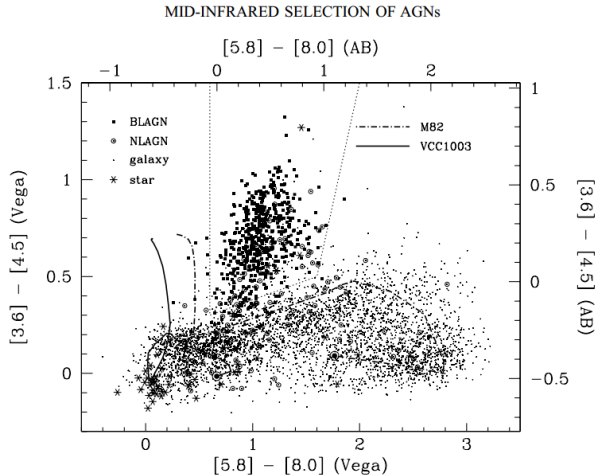


FIG. 4.— IRAC colors of spectroscopically identified objects from the AGES survey of the Boötes field. Axes indicate both the Vega and AB magnitude systems. Spectral classification of sources is noted in the upper left. The dotted line empirically separates active galaxies from Galactic stars and normal galaxies (Stern et al. 2005).

In a WISE pointing at high Galactic latitude, the vertical restriction eliminating cool, Galactic contaminants is also unnecessary. A shallow WISE pointing at high Galactic latitude would therefore be able to use only the two most sensitive wavelength bands for AGN selection (Stern et al. 2005). The WISE $[W1]-[W2]$ ($[3.6] - [4.5]$) color has been simulated for a variety of redshifts and AGN fractions by Assef et al. (2010), and the results (Fig. 5) motivate a simple $[W1]-[W2] \geq 0.8$ AGN selection criteria that works well for most sources.

The Cosmic Evolution Survey (COSMOS; Scoville et al. (2007)) is a 2 deg^2 field meeting both the equatorial and high galactic latitude requirements described above for contamination reduction. Additionally, the COSMOS field has been well-studied by many different instruments across the electromagnetic spectrum. The purpose of this paper is to determine the efficacy of the WISE AGN selection technique using the S-COSMOS (Sanders et al. 2007) survey with the Stern et al. (2005) IRAC selection criteria as a truth table. Furthermore, the multi-wavelength properties of WISE-selected AGN are examined, and the ability of WISE to discover obscured, type II AGN is evaluated. This paper is a reproduction of the work contained in Stern et al. (2012).

2. AGN SELECTION USING WISE

2.1. Identifying IRAC Counterparts

In order to use the S-COSMOS survey as a truth table, the analysis must be restricted to sources detected by both WISE and IRAC in the COSMOS field. We begin by applying a set of filters to the WISE and S-COSMOS source catalogs to remove spurious or saturated detections. These sources are then cross-referenced, and only those sources detected in both surveys are retained.

WISE sources with $149^\circ < \text{RA} < 151^\circ$ and $1^\circ < \text{DEC} < 3^\circ$ were downloaded from the March 14, 2012 All-Sky Data Release available on the Infrared Science Archive (IRSA). This region was defined to completely contain the COSMOS field so as not to miss any boundary sources. Our analysis is restricted to sources with a

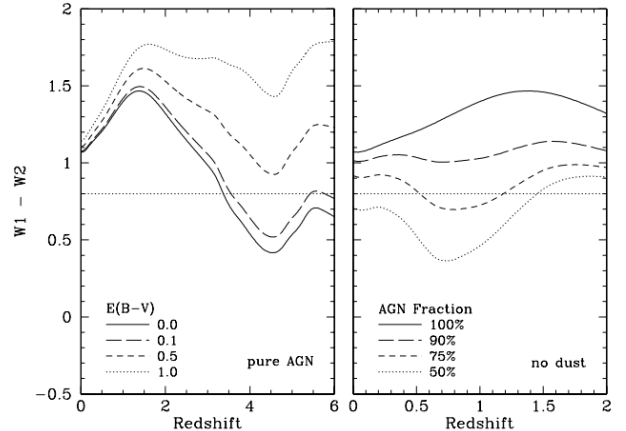


FIG. 5.— Model colors of AGN versus redshift based on simulations of Assef et al. (2010). The dotted line shows the color criteria of $[W1]-[W2] \geq 0.8$. The simulations were done based on level of extinction within the source (left) and the fraction of total luminosity due to the AGN rather than (Stern et al. 2012)

signal-to-noise ratio $\gtrsim 10\sigma$ in the W2 band, corresponding to a 15.05 mag depth. Sources deblended with more than two components (i.e. $NB > 2$) were removed from our analysis, as well as any sources flagged as spurious detections of nearby bright sources (i.e. $ccflags \neq 0$). 7684 WISE sources were identified satisfying these filters.

IRAC sources within the COSMOS field are contained in the S-COSMOS catalog (`scosmos_irac_200706.tbl`) available from IRSA. IRAC sources were sent through a similar filtering process to the WISE data; sources with a SExtractor flag not equal to 0 were removed, as well as any sources with negative flux values in any of the four IRAC bands, and saturated stars were removed by requiring $[3.6] \geq 11$. For each of the 7684 WISE sources in our search region, the resultant list of S-COSMOS sources was searched for counterparts using a conservative 1 arcsecond matching radius (see Fig. 7 later in the paper). IRAC counterparts for 2187 of the WISE sources were found. None of the WISE sources were found to have more than one S-COSMOS counterpart.

2.2. AGN Selection with IRAC and WISE

The appropriate AGN color selection criteria were applied to each survey. The WISE-selected AGN were cross-referenced with the IRAC-selected AGN to determine the efficacy of the simple WISE selection technique. This was quantified by completeness, the fraction of IRAC-selected AGN also selected by WISE, and reliability, the fraction of WISE-selected AGN also selected by IRAC.

Each of the 2187 WISE sources having an IRAC counterpart was classified using both the Stern et al. (2005) IRAC criteria and the WISE $W1-W2$ color criteria defined in the introduction. Fig. 6 shows an IRAC color-color diagram with the selection results indicated by plot symbol. Sources satisfying the IRAC color criteria are taken to be the truth sample of AGN, those satisfying the WISE criteria are WISE AGN candidates. Sources satisfying the requirements for both IRAC and WISE are confirmed WISE-selected AGN. Any sources identified by WISE that fail to meet the IRAC criteria

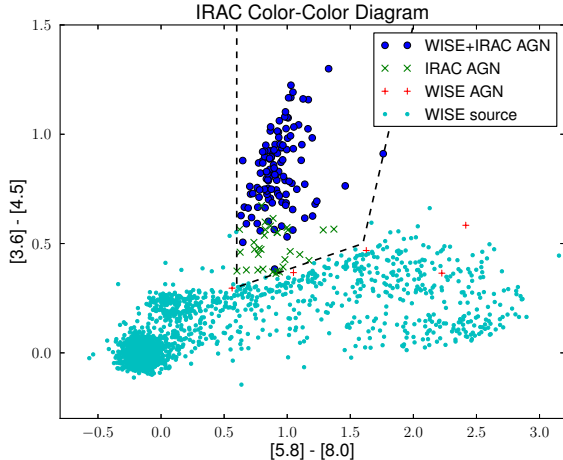


FIG. 6.— IRAC color-color diagram of WISE-selected sources having S-COSMOS counterparts. Those sources classified as AGN using both IRAC and WISE selection criteria are indicated by larger blue circles. Those selected as AGN only by IRAC criteria are shown with a green \times , and those selected only by WISE criteria are shown by a red $+$. Sources not classified as AGN by any criteria are indicated by cyan dots. Stern et al. (2005) IRAC selection criteria are indicated by the dashed lines.

are considered contaminants.

148 of the 2187 WISE-IRAC matched sources are classified as AGN according to the Stern et al. (2005) IRAC selection criteria, while 123 are classified as AGN according to the $W1-W2 \geq 0.8$ criteria. Of the 123 sources identified by WISE, 116 also meet the IRAC criteria. Taking the IRAC AGN as the truth sample, the completeness of the WISE selection is calculated as the AGN detected by WISE divided by those detected by IRAC:

$$\text{Completeness} = 116/148 = 0.784.$$

The reliability of the selection is defined as the number of true AGN divided by the total number of candidates:

$$\text{Reliability} = 116/123 = 0.943.$$

3. MULTI-WAVELENGTH PROPERTIES OF WISE AGNS

The multi-wavelength properties of the detected AGN were examined using publicly available catalogs of X-ray and radio observations of the COSMOS field. Public catalogs of point sources detected by XMM-Newton (Jansen et al. 2001), Chandra (Weisskopf et al. 2000), and VLA (Thompson et al. 1980) in the COSMOS field were used to investigate the multi-wavelength properties of the AGN detected with the simple WISE color criteria. The observations by XMM-Newton, Chandra, and the VLA were made public with point source catalogs available through IRSA. Taking the sources which satisfied both the WISE and IRAC criteria as the true AGN, those true AGN were positionally matched to sources detected in other wavelengths. Matching radii were chosen as the ~ 3 sigma level of the quoted position error of all objects in each source catalog, as illustrated in Fig. 7. To identify the unobscured, type I AGN in our sample, we cross-reference our sources with the Sloan Digital

Sky Survey (SDSS; York et al. (2000)) Quasar Catalog (Schneider 2006).

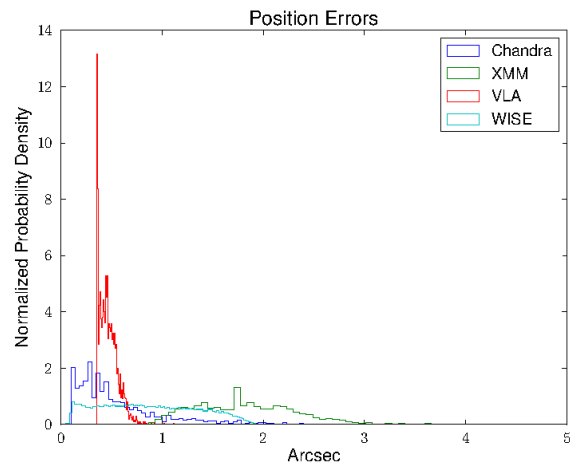


FIG. 7.— Quoted positional error of sources for the considered instrument surveys of the COSMOS field

3.1. Radio Properties of WISE Detected AGN

The VLA observed the COSMOS field at 20 cm for 350 hrs in the A-array with a resolution of $1''.5$ and $\sim 11 \mu\text{Jy}$ sensitivity (Schinnerer et al. 2007). The catalog contains a total of 2864 sources within the COSMOS field. Using a $1''.5$ matching radius, we found 293 positionally matched sources in the WISE catalog, 50 being identified as AGN by WISE and IRAC criteria (43% of WISE and IRAC-selected AGN). The 43% of WISE and IRAC-selected AGN are illustrated in Fig. 8, where the dashed line corresponds to the WISE color criterion of $[W1]-[W2] \geq 0.8$.

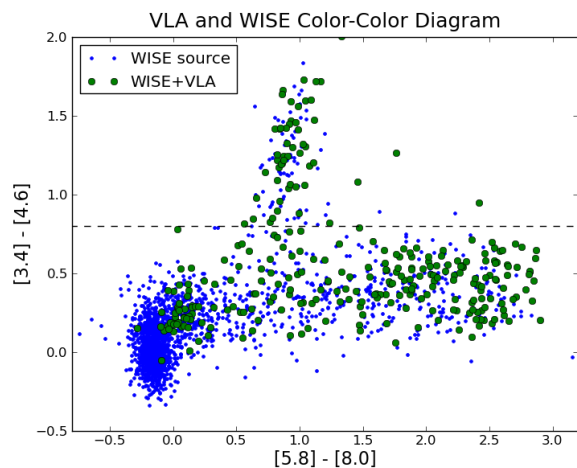


FIG. 8.— Color-color diagram showing the sources detected by WISE and by WISE+VLA. The dashed line denotes the color criterion for WISE AGN selection

3.2. X-Ray Properties of WISE Detected AGN

3.2.1. XMM-COSMOS Observations

XMM-Newton (XMM-COSMOS; Hasinger et al. (2007)) observed the entire COSMOS field to medium (60 ks) depth in the 0.5–2, 2–4.5, and 4.5–10 keV bands to an equivalent overall flux limit of 7×10^{16} ergs cm^{-2} s^{-1} . The catalog contains a total of 1887 sources within the COSMOS field. Using a matching radius of $3''.5$, we found 180 of those 1887 sources positionally matched to sources in the WISE catalog, 86 being identified as AGN by WISE and IRAC criteria (74% of WISE and IRAC-selected AGN). Fig. 9 shows the sources detected by WISE and by WISE and XMM-Newton. Different from the radio counterparts of WISE sources, sources along the vertical extension seem to preferentially have detectable X-ray counterparts, suggesting that active nuclei are more likely emitters of X-ray radiation than normal galaxies (as expected). Those sources below but close to the WISE selection cutoff detected by XMM-Newton might be good followup candidates as possible AGN sources missed by the color selection.

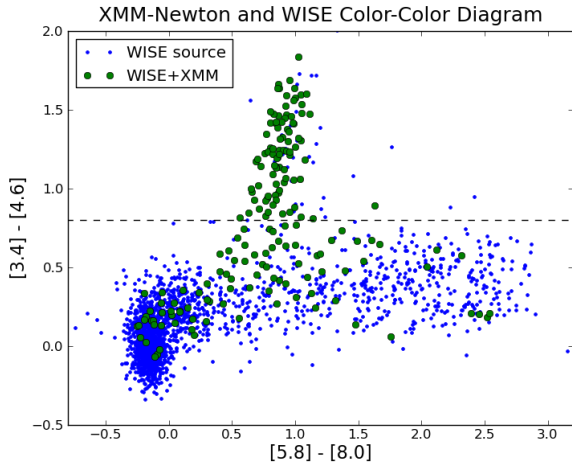


FIG. 9.— Color-color diagram showing the sources detected by WISE and by WISE+XMM-Newton. The dashed line denotes the color criterion for WISE AGN selection

3.2.2. Chandra-COSMOS Observations

The Chandra-COSMOS (C-COSMOS; Elvis et al. (2009)) survey imaged the central 0.5 deg^2 of the COSMOS field with an effective exposure time of 160 ks per position and an outer 0.4 deg^2 with an effective exposure time of 80 ks per position. The limiting source detection depths are 1.9×10^{-16} erg cm^{-2} s^{-1} in the soft (0.5–2 keV) band, 7.3×10^{-16} erg cm^{-2} s^{-1} in the hard (2–10 keV) band, and 5.7×10^{16} erg cm^{-2} s^{-1} in the full (0.5–10 keV) band. A $2''.5$ matching radius was used to positionally match sources between the WISE and Chandra catalogs. Because the C-COSMOS observations do not cover the entire 2 deg^2 field, source matching was restricted to only WISE sources that fell within the observational field of C-COSMOS (defined by corners at $[10^h 02^m 45^s, +02^\circ 26' 47'']$, $[09^h 59^m 11^s, +02^\circ 46' 45'']$, $[09^h 57^m 54^s, +01^\circ 53' 00'']$, $[10^h 01^m 23^s, +01^\circ 33' 59'']$). Of the 48 WISE detected AGN in the C-COSMOS field, 39

were also detected by Chandra as can be seen in Fig. 10. Similar to XMM-Newton counterparts, one observes a clustering of X-ray detections around the vertical extension on the color-color plot. Chandra deep fields are not expected to detect AGN with hydrogen column densities above $10^{23.5}$, therefore the 9 AGN sources undetected by Chandra are strong candidates for heavily obscured AGN with hydrogen column densities above this limit.

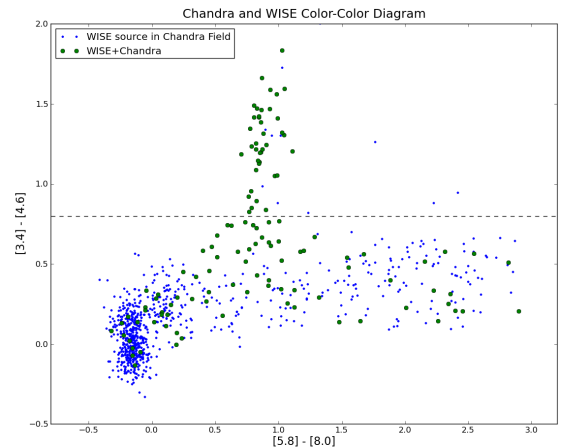


FIG. 10.— Color-color diagram showing the sources detected by WISE and by WISE and Chandra limited to the Chandra C-COSMOS field of view. The dashed line denotes the color criteria for WISE AGN selection

3.2.3. SDSS Quasar Survey Matching

In order to estimate the ratio of type II to type I AGN selected by WISE, we cross referenced our WISE-selected AGN with the SDSS Quasar Survey. The SDSS quasar catalog, available from the SDSS website, was searched for positional matches to our source list using a $2''$ matching radius based on the astrometric accuracy of SDSS. Of our 123 WISE-selected AGN, 46 were identified as type I quasars. We assume the other 77 WISE-selected AGN to be obscured, type II AGN.

3.3. Alternative WISE Pointings

Due to the isotropy of the XRB, it is expected that the density of WISE-selected AGN to a 15.05 mag W2 depth at high Galactic latitude pointings would be statistically consistent with that of the COSMOS field. Source catalogs for 4 deg^2 equatorial WISE pointings located at $(195^\circ, 0^\circ)$, $(345^\circ, 0^\circ)$, $(165^\circ, 0^\circ)$, $(10^\circ, 0^\circ)$, and $(60^\circ, 0^\circ)$ were filtered for AGN using the WISE color selection criteria. The resulting AGN densities were 77.25, 53.75, 54.75, 55.5, and 61.5 AGN/ deg^2 , respectively. Combining these measurements with the 61.5 AGN/ deg^2 in the COSMOS field, we find a best fit constant of 59.87 AGN/ deg^2 with a reduced χ^2 of 1.11. We find a 0.353 p-value for rejecting the hypothesis that the density is constant, much too high to reject.

4. DISCUSSION

The completeness and reliability of the simple WISE color AGN-selection technique are 78% and 94%,

respectively. This demonstrates the usefulness of the WISE survey as an AGN finder. Depending on the preference of the observer, an adjustment of the 0.8 cutoff value can shift the technique toward completeness or reliability. A higher cutoff reduces the probability of selecting red inactive galaxies, but sacrifices completeness by eliminating borderline AGN. Conversely, a lower cutoff increases completeness at the expense of including a higher number of contaminant galaxies. The consistency of AGN densities at equatorial and high galactic latitudes implies the selection criterion works well for large portions of sky with similarly shallow WISE coverage and low galactic contamination.

Of the WISE and IRAC-selected AGN, 49% were found to have detectable radio counterparts. This is higher than the expected value of 10% of AGN being radio-loud (Stern et al. 2000). However, some of the sources detected may be less luminous than the cutoff level to be considered radio-loud; to determine the true number of radio-loud AGN detected it would be necessary to apply a luminosity cutoff to each source individually. Additionally, the matching radius used in this study may overestimate the number of radio counterparts by using a $1''.5$ radius for sources with significantly smaller positional uncertainties.

74% of the WISE-selected AGN were detected by XMM-Newton while the deep Chandra observations detected 81% of the WISE AGN sources within the C-COSMOS field. Those sources not detected in the X-ray bands may be heavily obscured AGN and are good candidates for hard X-ray followup observations. The recently launched Hard X-ray telescope NuStar (Harrison et al. 2010) is sensitive in the 6–79 keV energy band and will allow the study of these most heavily obscured AGN.

By integrating Fig. 1 above and below the Chandra deep field detection cutoff at $N_H = 10^{23.5} \text{ cm}^{-2}$, one expects Chandra deep pointings to detect $\sim 64\%$ of AGN sources, or a 1.78:1 ratio of sources below to sources above the N_H cutoff. By taking the number of WISE sources detected by Chandra as being below the N_H cutoff, this study finds a 4.33 ratio of sources below to sources above the N_H cutoff. In order to correct for the intrinsic bias of the IRAC truth sample, these results were normalized to the percentage of sources of type I and type II AGN detected by IRAC (90% and 40%, respectively). This normalization recovers a ratio of 1.93 which is in better agreement with the predicted ratio of 1.78.

The mean $i - [4.6]$ color of the 46 WISE-selected AGN identified as type I quasars by SDSS is 4.75. Given the 15.05 magnitude W2 depth of our WISE pointing, we estimate a i band depth of 19.8. Richards et al. (2006) used SDSS and the Two Degree Field QSO Redshift Survey (2QZ; Boyle et al. (2000)) to determine the number density of type I quasars as a function of i band depth. They find ~ 20 type I quasars per deg^2 at the same i band depth. This is roughly consistent with the 23 type I quasars per deg^2 we find based on matching to the SDSS quasar catalog. Assuming the remainder of the 61.5 AGN per deg^2 selected by WISE to be type II AGN, we find a 2.08:1 ratio of type II to type I AGN. However, given that the IRAC selection technique only selected 91% and 40% of AGES-identified type I and type II AGN, we normalize this ratio to 4.68:1. While higher than the 3:1 ratio predicted by Treister & Urry (2005), this ratio is reasonable. The increased density of obscured AGN implied by these results support predictions of a large population of missing type II AGN, consistent with the current understanding of the XRB origin.

REFERENCES

- Abazajian, K. N., Adelman-McCarthy, J. K., Agüeros, M. A., et al. 2009, *ApJS*, 182, 543
- Assef, R. J., Kochanek, C. S., Brodwin, M., et al. 2010, *ApJ*, 713, 970
- Bauer, F. E., Alexander, D. M., Brandt, W. N., et al. 2004, *AJ*, 128, 2048
- Boyle, B. J., Shanks, T., Croom, S. M., et al. 2000, *MNRAS*, 317, 1014
- Brandt, W. N., & Hasinger, G. 2005, *ARA&A*, 43, 827
- Blain, A., et al. 2012, *ApJ*, submitted
- Comastri, A., Setti, G., Zamorani, G., & Hasinger, G. 1995, *A&A*, 296, 1
- Dickinson, M., Giavalisco, M., & GOODS Team 2003, *The Mass of Galaxies at Low and High Redshift*, 324
- Fazio, G. G., Hora, J. L., Allen, L. E., et al. 2004, *ApJS*, 154, 10
- Elvis, M., Civano, F., Vignali, C., et al. 2009, *ApJS*, 184, 158
- Fabian, A. C., & Barcons, X. 1992, *ARA&A*, 30, 429
- Giacconi, R., Gursky, H., Paolini, F. R., & Rossi, B. B. 1962, *Physical Review Letters*, 9, 439
- Gilli, R., Risaliti, G., & Salvati, M. 1999, *A&A*, 347, 424
- Harrison, F. A., Boggs, S., Christensen, F., et al. 2010, *Proc. SPIE*, 7732,
- Hasinger, G., Burg, R., Giacconi, R., et al. 1998, *A&A*, 329, 482
- Hasinger, G., Cappelluti, N., Brunner, H., et al. 2007, *ApJS*, 172, 29
- Jannuzi, B. T., & Dey, A. 1999, in *ASP Conf. Ser.* 191
- Jansen, F., Lumb, D., Altieri, B., et al. 2001, *A&A*, 365, L1
- Khachikian, E. Y., & Weedman, D. W. 1974, *ApJ*, 192, 581
- Kochanek, C. S., Eisenstein, D. J., Cool, R. J., et al. 2012, *ApJS*, 200, 8
- Madau, P., Ghisellini, G., & Fabian, A. C. 1994, *MNRAS*, 270, L17
- Magorrian, J., Tremaine, S., et al. 1998, *AJ*, 115, 2285
- Mortlock, D. J., Warren, S. J., Venemans, B. P., et al. 2011, *Nature*, 474, 616
- Pompilio, F., La Franca, F., & Matt, G. 2000, *A&A*, 353, 440
- Richards, G. T., Fan, X., Newberg, H. J., et al. 2002, *AJ*, 123, 2945
- Richards, G. T., Strauss, M. A., Fan, X., et al. 2006, *AJ*, 131, 2766
- Rowan-Robinson, M. 1977, *ApJ*, 213, 635
- Sanders, D. B., Salvato, M., Aussel, H., et al. 2007, *ApJS*, 172, 86
- Schneider, P. 2006, *Extragalactic Astronomy and Cosmology*, by Peter Schneider. Berlin: Springer, 2006.,
- Schinnerer, E., Smolčić, V., Carilli, C. L., et al. 2007, *ApJS*, 172, 46
- Schmidt, M., & Green, R. F. 1983, *ApJ*, 269, 352
- Scoville, N., Aussel, H., Brusa, M., et al. 2007, *ApJS*, 172, 1
- Seward, F. D., & Charles, P. A. 1995, *Exploring the X-Ray Universe*, by Frederick D. Seward and Philip A. Charles, pp. 414. ISBN 0521437121. Cambridge, UK: Cambridge University Press, November 1995.
- Stern, D., Djorgovski, S. G., Perley, R. A., de Carvalho, R. R., & Wall, J. V. 2000, *AJ*, 119, 1526
- Stern, D., Eisenhardt, P., et al. 2005, *ApJ*, 631, 163
- Stern, D., Assef, R. J., Benford, D. J., et al. 2012, *ApJ*, 753, 30
- Thompson, A. R., Clark, B. G., Wade, C. M., & Napier, P. J. 1980, *ApJS*, 44, 151
- Treister, E., & Urry, C. M. 2005, *ApJ*, 630, 115
- Tremaine, S., Gebhardt, K., et al. 2002, *ApJ*, 574, 740
- Weisskopf, M. C., Tananbaum, H. D., Van Speybroeck, L. P., & O'Dell, S. L. 2000, *Proc. SPIE*, 4012, 2
- Werner, M. W., et al. 2004, *ApJS*, 154, 1

Worsley, M. A., Fabian, A. C., Barcons, X., et al. 2004, MNRAS, 352, L28
Worsley, M. A., Fabian, A. C., Bauer, F. E., et al. 2005, MNRAS, 357, 1281

Wright, E. L., Eisenhardt, P. R. M., Mainzer, A. K., et al. 2010, AJ, 140, 1868
York, D. G., Adelman, J., Anderson, J. E., Jr., et al. 2000, AJ, 120, 1579